

An Optimization of Nanostructure Aluminum on Porous Silicon at Different Aluminum Thickness

N. M. Ramli¹, M. K. Ahmad^{1,*}, M. A. D. Adam¹, F. Mohamad¹, N. Nafarizal¹, C. F. Soon¹, A. S. Ameruddin², A. B. Faridah², M. Shimomura³, and K. Murakami³

¹Microelectronic and Nanotechnology – Shamsuddin Research Centre (MiNT-SRC) Faculty of Electrical and Electronic Engineering, Universiti Tun Hussein Onn Malaysia, 86400 Parit Raja, Batu Pahat, Johor, Malaysia.

²Department of Science, Faculty of Science, Technology, and Human Development, Universiti Tun Hussein Onn Malaysia, 86400 Parit Raja, Batu Pahat, Johor, Malaysia.

³Department of Engineering, Graduate School of Integrated Science and Technology, Shizuoka University, 432-8011 Hamamatsu, Shizuoka, Japan

Abstract: The growth of aluminum nanostructure was conducted on porous silicon substrate by depositing a layer of aluminum via thermal evaporation method. The deposition process of the aluminum nanostructure was under the annealing temperature at 350°C for 1 hour. The weight of aluminum was varied for each sample in order to obtain different thickness of aluminum deposited on the sample. The weight of aluminum used in this experiment were 12mg, 18mg, 50mg and 74mg with the corresponding aluminum thickness deposited of 112nm, 163nm, 205nm and 332nm. Characterization on the morphology of the sample are conducted by using Atomic force microscopy (AFM), Raman spectroscopy and IV measurements. Based on the result obtained, the optimum weight of aluminum was 50mg of aluminum since it is provide the higher conductivity value on the sample.

Keywords: Porous silicon, hydrofluoric acid, aluminum nanostructures, thermal evaporation method, Raman spectroscopy

1. Introduction

Aluminum nanostructure have been gaining the interest of researcher recently due to its high energy density and high heat reaction [1]. It's also know that aluminum nanostructure have high reactivity compared to microstructure aluminum, thus due to its versatility in application due to the mentioned characteristic, many current research are studying about nanostructure aluminum to benefit the future growth of technology[1][2]. Porous silicon can be produce by the process of electrochemical etching, the process uses hydrofluoric acid mixed with de-ionized water or ethanol or both[3][5]. The etching will be carried out with the base of the Teflon connected as anode the top electrode as cathode, with a constant current supply throughout the process[3]. Porous silicon can be fabricated from both n-type or p-type silicon wafers, the porous template or etched area of the silicon have a high nano to macro-porous surface area.

The pores on the porous silicon are the results of in homogenous dissolution of silicon surface by the hydrofluoric solution. Porous silicon are an interesting material, due to it's a kind nanostructure that involve the silicon substrate to act as a template or target. The silicon wafer have different characteristic from the conventional silicon wafer such as it has a tunable band gap of 1.8 to 2.2eV, higher surface area, higher reactivity and could potentially be a template for growing a nanostructure material. Porous silicon are currently being research for its

potential on the optoelectronics due to the tunable band gap[3][4][5]. Research have state that different amount of current density applied will produce a varying result of porous intensity and the porous layer thickness[4]. Refer to table 1.1 shows a current density effect on porous intensity and thickness of porous silicon formed.

Table 1.1: Current density effect on porous intensity and thickness of porous silicon formed.
(M.H.F. Suhaimi, M. Rusop, and S. Abdullah, 2013)

| Current Density J(mA/cm ²) | Porosity (%) | Thickness (μm) |
|---|--------------|----------------|
| 20 | 71.43 | 5.86 |
| 25 | 77.91 | 5.51 |
| 30 | 82.35 | 5.56 |
| 35 | 80.65 | 5.29 |
| 40 | 78.10 | 5.47 |

The porous intensity are determine by the following formula: $porosity(\%) = \frac{mass_1 - mass_2}{mass_1 - mass_3} \times 100\%$.

Where $mass_1$ is the mass of silicon before etch, $mass_2$ is the mass of silicon after etch and $mass_3$ is the mass of silicon after porous are removed. At first, silicon porous was studied for its application in microelectronics as an insulating material. But soon after the discovery of its photoluminescence under ultraviolet excitation many studies have been moving towards optoelectronics, such as its application towards display technologies and chemical sensing. From recent studies, the optical properties of silicon porous are applied as an anti-reflecting coating, biosensors and interference filters [6].

2. Fabrication Process Flow

Aluminum nanostructure will be fabricated on top of a P-type silicon wafer porous template. The optimization is performed during the deposition of aluminum, whereby the thickness of the aluminum are deposited with different parameter across multiple samples. The thickness parameter are controlled by the weight of the aluminum sources, the parameters of the weight used are 12mg, 18mg, 50mg and 74mg.

Ultrasonic Cleaning

Silicon wafer cleaning will be treated using the ultrasonic technique. The technique uses a chemical bath consisting a mixture of 1 part acetone, 1 part ethanol and 1 part de-ionized water (1 acetone: 1 ethanol: 1 DI water). The equipment being used are Power sonic 405 with the sonic level of two for a duration of 10 minutes.

Porous Silicon

The method on fabricating the porous silicon uses the electrochemical etching. Electrochemical etching requires a Teflon cell to hold the wafer and expose parts of the wafer with HF acid to chemically etch the wafer surface. The reaction is further enhanced with the aid of current source flowing through the electrodes, where the wafer or the base of the Teflon cell act as an anode while the tungsten rod acts as a cathode. The mixture of the acid uses a ratio of 1 part of HF acid and 20 parts of de-ionized water (1 HF: 20 DI water). The current source are generated using Keithley source meter series 2420 at constant rate of 20 mA for 5 hours. The resulting porous silicon is then rinse with DI water and left to dry. Figure 2.1 shows the setup of equipment to produce the porous silicon.

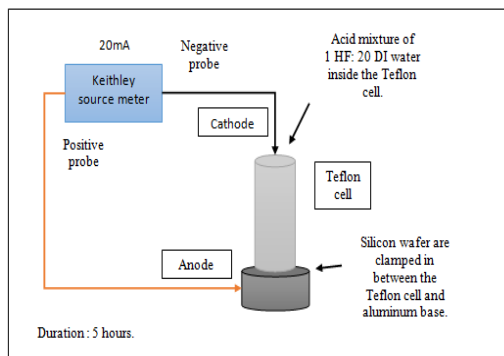


Figure 2.1: The equipment setup for the electrochemical etching.

Aluminium Deposition

Deposition of Aluminum thin film on the silicon porous substrates performed by using the thermal evaporation method. This method vaporizes the aluminum source in vacuum environment which will be condensed on the silicon porous substrate surface to produce a thin layer of aluminum on top of the substrate. During this process, the amount of aluminum deposit at the surface will be varied by their thickness. The thickness parameter to achieve are thickness of $\leq 140\text{nm}$, $\leq 160\text{nm}$, $\leq 210\text{nm}$ and $\leq 320\text{nm}$. To control the aluminum thickness the aluminum source weight must be control, thus four weight parameter was chosen which is 12mg, 18mg, 50mg, and 70mg. The purpose of this variance are to experiment on relation of thickness of aluminum deposit could manipulate the outcomes of the final product on the nanostructure and whether or not the aluminum nanostructure characteristic and density could be improved by increasing the thickness of aluminum during deposition process. Figure 2.2 (a) shows the thermal evaporator machine and figure 2.2 (b) shows the sample of aluminum deposited on porous silicon.

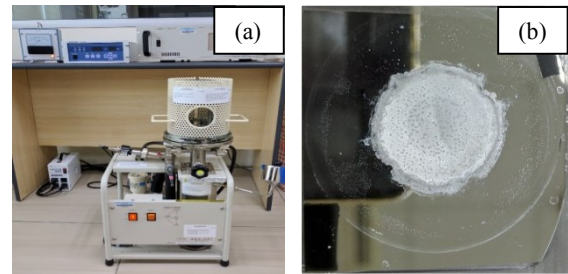


Figure 2.2 : (a) Thermal Evaporator machine used for thin film deposition and (b) The sample of aluminum deposited on porous silicon.

Annealing

The annealing process involves the heating of the sample to potentially growth an aluminum nanostructure, the heating process involve the usage of a furnace and simply heating the aluminum deposited on the silicon porous could potentially growth the nanostructure due to the heat stress from the process. The annealing process is performed for 1 hour at the temperature of 350°C across all sample.

3. Results and Discussion

Atomic Force Microscope (AFM)

The samples are characterized by using AFM (MODEL: XE-100) . The Figure 3.1 shows the sample of 2D surface morphology while figure 3.2 shows the 3D surface representation. The result shows that as the thickness increases the size of the particles will increase except for the case of thickness 205nm of which a 50mg of aluminum was deposited. The particles on 50mg was much finer and the volume of particle is higher than that of other parameter. In the case of 112.84nm which uses an aluminum deposit weighting of 12mg, the aluminum thin film layer was too thin and exposes the silicon surface that

have been proven by Raman characterization. Since the AFM image of 12mg sample characteristic differs from other sample, it is possible that the image of the 12mg sample represents the image for silicon porous with transparent layers of aluminum. To compare the difference between sample of 12mg and the other three sample, the sample other than 12mg have been fully covered with aluminum and possibly the nanostructure itself.

The other three sample shows a good grain boundary which did not exist on the sample 12mg, further reinforcing my statement of which sample 12mg surface scan image is the silicon porous surface with thin and almost transparent layer of aluminum. Sample 18mg scan have a scattered pattern and the particle size is bigger that the size of sample 12mg and the particle seems to congest and converge with each other forming a groups of highly concentrated particle region. The case of particle forming concentrated convergence of particle region are similar for the sample of 18mg, 50mg and 74mg, this phenomenon leads to hypothesis that concludes with modest amount of aluminum on the film layer, the nanostructure could form a dense particle region formed by heat displacement and a template of porous silicon. While with not enough aluminum on the thin film the particle will not conjoined and the image produce could probably be the silicon porous and not the aluminum nanostructure. As for the case of sample 74mg, the sample may be forming a nanostructure of nanoflower due to the resemblance of the shape from the particle of the aluminum nanostructure.

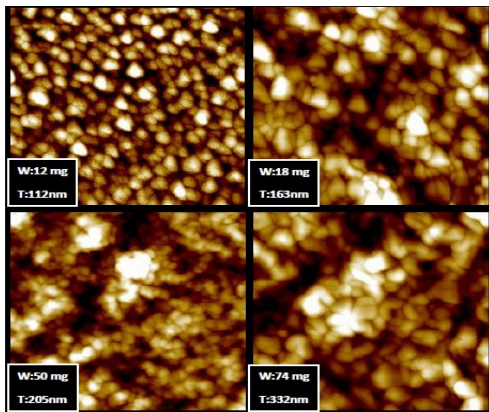


Figure 3.1: AFM image of all sample on 2D surface representation.

Further discussion on the 3D result of the surface for thickness 112.84nm with the weight 12 mg of the aluminum source. The average roughness of the sample is 2.914nm and the max region of 15.422nm. For sample thickness of 163.22nm, the weight of the aluminum deposit used was 18mg and the average roughness of the sample is 4.183nm while the max region is 18.169nm. Next for the thickness of 205.24nm the weight of the aluminum deposit is 50mg while the average roughness is 8.087nm and the max region is 50.685nm. Lastly, for the thickness of 332.13nm, the weight of aluminum deposit is 74mg resulting in an average roughness of 8.564nm and max region of 32.530nm. The max region stands for the

maximum displacement on Y-axis of the sample, it represents the highest point of a grain particle displaced from point 0.

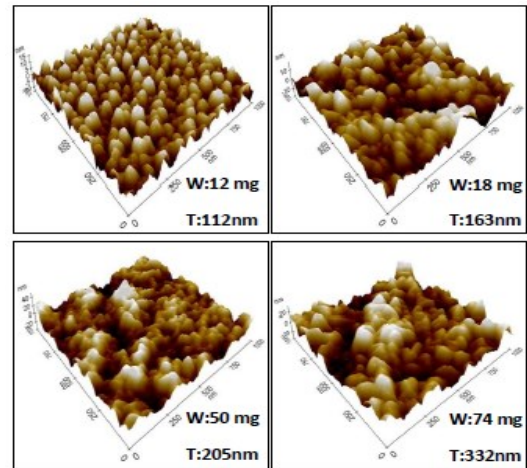


Figure 3.2: AFM image of all sample on 3D surface representation.

To simplify the results, Table 3.1 shows the comparison of each samples. The result of weight of aluminum deposit versus the average roughness obtained shows to have exponentially high growth in the mid parameter between 18mg and 50mg, with low increment of roughness on parameter of 50mg to 74mg. The high increment on the middle of the data are probably due to the vast different between the weight of sample 18mg and sample 50mg, thus producing a higher thickness of thin film which could potentially cause higher roughness on the surface. Furthering the discussion on the value of weight of aluminium deposit versus the max region or max displacement, this value produces an abnormal pattern of which for the first three parameters of 12mg, 18mg, and 50mg produces an increment of displacement in nanometer while for the parameter of 74mg the graph decreases to from point 50nm to 32nm. This is due to the non-uniform surface of the aluminum deposited.

Table 3.1: The comparison of all parameters on AFM of each sample.

| Thickness (nm) | Weight of aluminium (mg) | Average roughness (nm) | Max displacement(nm) |
|----------------|--------------------------|------------------------|----------------------|
| 112.84 | 12 | 2.194 | 15.422 |
| 163.22 | 18 | 4.183 | 18.169 |
| 205.24 | 50 | 8.087 | 50.685 |
| 332.13 | 74 | 8.564 | 32.530 |

Furthering the discussion on the result of weight of aluminum deposit versus the max region or max displacement, the result produces an abnormal pattern of which for the first three parameters of 12mg, 18mg, and

50mg produces an increment of displacement in nanometer while for the parameter of 74mg the graph decreases to from point 50nm to 32nm. To conclude the results of the table, as the thickness increase, the roughness of the sample increase. While the max region relation is the same excluding the sample of 74mg where the value is lower than the result of 50mg.

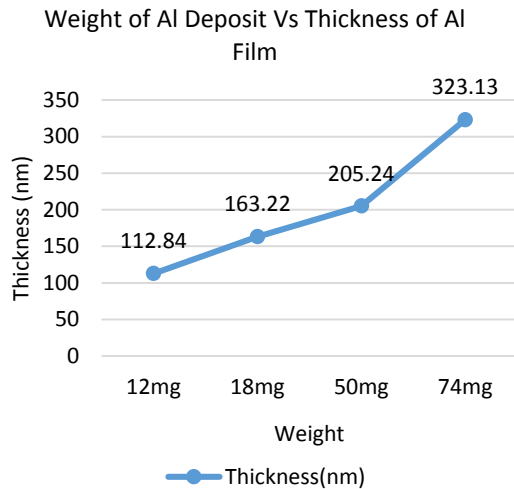


Figure 3.3: Graph weight of aluminum deposit Vs Thickness of Al Film.

The graph of weight of aluminum deposit versus the thickness of thin film as shown in Figure 3.3 shows that the thickness of thin film produce is directly proportional to the weight of aluminum deposit, thus we can conclude that the weight of aluminum is the manipulating factor for the thickness of aluminum thin film deposited.

Table 3.2: The Average Grain Size and its standard deviation.

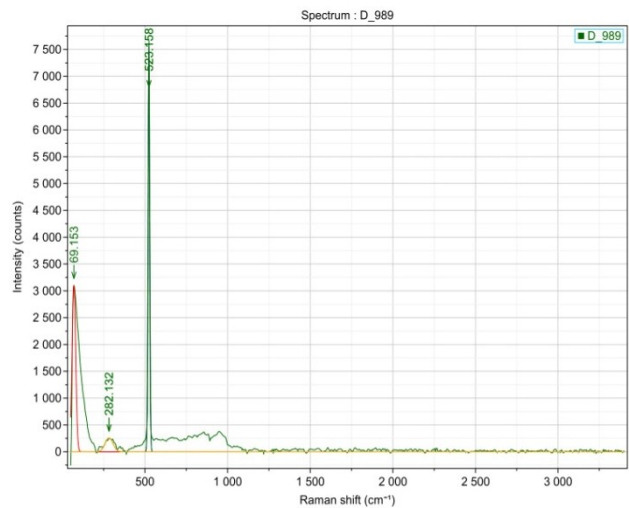
| Weight of aluminium (mg) | Grain size in one line (nm) | | | Average grain size (nm) | Standard deviation, σ |
|--------------------------|-----------------------------|----------------|----------------|-------------------------|------------------------------|
| | G ₁ | G ₂ | G ₃ | | |
| 12 | 43.4 | 52.6 | 55.5 | 50.5 | 5.16 |
| 18 | 66.7 | 62.5 | 62.5 | 63.9 | 1.97 |
| 50 | 50.0 | 45.5 | 38.5 | 44.7 | 4.73 |
| 74 | 71.4 | 66.7 | 62.5 | 66.9 | 3.64 |

The average grain size of each sample are shown on table 3.2, the grain size are manually calculated using the line method. The method uses a line drawn on the AFM image, by marking the intersection of the drawn line and the grain boundary, the grain size on a line can be calculate by dividing line length by total intersection of the line boundary.

RAMAN Spectroscopy

Based on the Raman Spectroscopy (MODEL: XploRA Plus) HORIBA Instruments (S) Pte Ltd characterization result, for sample of 12mg, the thickness of aluminum is too thin possibly exposing the silicon substrate thus the reading of Raman shift shows that it have detected a silicon porous spectrum. The silicon porous spectrum is at 521cm^{-1} [1], from the figure below the Raman spectrum detects a silicon porous at the range of 523cm^{-1} . Proving that the surface of the porous silicon is not fully coated with aluminum, as such the aluminum appears to be semi-transparent and exposing the silicon porous substrate in the Raman spectrum.

Figure 3.4 shows the Raman spectrum of sample 12mg. For the other 3 sample Raman was unable to identify any aluminum oxide or porous silicon, since Raman spectroscopy are unable to determine the Raman shift of aluminum due to aluminum being a metal, we can conclude that the surface is covered by pure aluminum not aluminum oxide. As for the result of the optical image on the Raman spectroscopy, there were no actual image that forms an image of aluminum nanostructure except for the case of sample 74mg. This is because Raman microscope are low in resolution in this case $20\mu\text{m} \times 20\mu\text{m}$, whereby compared to AFM that scans the sample at $1\mu\text{m} \times 1\mu\text{m}$.



Raman excels in determining the elements on a sample surface by using the Raman spectra.

Figure 3.4: Raman spectrum of sample 12mg

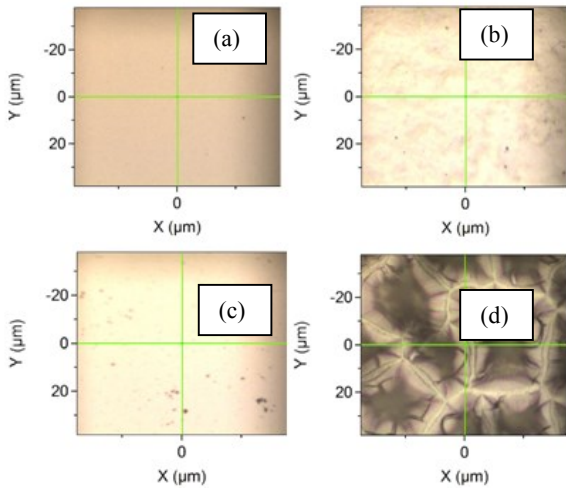


Figure 3.5: Raman microscopy image of each sample.

Figure 3.5 shows the comparison of Raman microscopy images. While other sample (a), (b), and (c) have no actual distinguishable characteristic on the microscopy images, sample 74mg (d) shows a pattern on the surface of the substrate during RAMAN microscopy. The sample forms a kaleidoscope like pattern on the optical microscopy but show no abnormal readings on the RAMAN spectra. While there are no actual value for aluminum or any metal as a reference on RAMAN spectra scan, the result of the sample scanning prove to show that the Raman spectra for aluminum could be ranging from 70 to 80 cm^{-1} while Raman spectra of silicon porous is 521 cm^{-1} .

IV measurement

The IV measurement is conducted using the four point probe (MODEL: Pro4-440N) LUCAS LAB, the measurement is conducted on 3 points inside the porous region. The measurement is then calculated for average result.

Table 3.3 : The 4 point probe average results.

| Sample | Average sheet resistant, Rsh (Ω/sq) | Average resistivity, ρ (ohm-cm) | Conductivity (S/m) |
|--------|---|--------------------------------------|-----------------------|
| 12 | 4.81×10^{11} | 5.43×10^6 | 1.84×10^{-7} |
| 18 | 1.57×10^{11} | 2.56×10^6 | 3.90×10^{-7} |
| 50 | 9.69×10^9 | 1.99×10^5 | 5.02×10^{-6} |
| 74 | 3.93×10^{10} | 1.30×10^6 | 7.69×10^{-7} |

Table 3.3 shows the 4 point probe average results. The sheet resistance of the sample decreases as the thickness of the aluminum thin film increases. Sample 50mg have the lowest average sheet resistance compared to the other sample, 50mg sample have been identified in AFM to have more nanostructure aluminum compared to the other three sample. Thus 50mg being the lowest sheet resistance could

possibly due to the relation of its nanostructure being more concentrated and most finest between other sample. From the result obtained in Raman spectroscopy, there no is no need to be characterize by using X-Ray Diffractometer (XRD) or E-Beam Lithography (EDX) since it will provide same information as Raman Spectroscopy technology.

4. Summary

Results of fabrication an aluminum nanostructure on top of the silicon porous substrate is obtained. The porous silicon were able to develop by using the electrochemical etching with current supply of 20 mA for a duration of 5 hours, particles of aluminum are shown to increase in size with the increase of aluminum thickness. The research shows that the thickness of aluminum produces different particle count and size, as the thickness increase the size of the particle increase except for the case of sample 50mg. sample of 50 mg have the thickness of 205.24nm and produces the most particle count and have the smallest particle size. While the result of sample 12mg shows that thickness of 112.84 is too thin that during the characterize by Raman spectroscopy, silicon porous Raman shift was able to register on the Raman spectrum. To conclude the finding of this study, we would recommend using a thickness of ~200nm to optimize the particle density and size of the aluminum nanostructure.

References

- [1] N. Arora and B. R. Jagirdar, "Monodispersity and stability: case of ultrafine aluminium nanoparticles (<5 nm) synthesized by the solvated metal atom dispersion approach," *J. Mater. Chem.*, vol. 22, no. 18, p. 9058, 2012.
- [2] S. Shabana, S.H sonawane, V.Rangnathan, P.H. Pujjarwar, D.V. Pinjari, B.A. Bhanvase, P.R. Gogate, M. Ashokkumar "Improved synthesis of aluminium nanoparticles using ultrasound assisted approach and subsequent dispersion studies in di-octyl adipate," *Ultrason. Sonochem.*, vol. 36, pp. 59–69, 2017.
- [3] N. I. Rusli, H. Abdulgafour, Z. Hassan, F. K. Yam, N. K. Ali, A. M. Hashim, M. R. Mahmood, N. Nayan "ZnO Nanostructures Grown on Porous Silicon Substrate without Catalyst," *Int. Conf. Enabling Sci. Nanotechnol. 2012*, no. January, 2012.
- [4] M. H. Fadzilah Suhaim, M. Rusop, S. Abdullah "Porosity and Thickness Effect of Porous Silicon Layer on Photoluminescence Spectra," *Int. Conf. Technol. Informatics, Manag. Eng. Environ.* pp. 115–118, 2013.
- [5] S. Chandrasekaran, S. Vijayakumar, T. Nann, and N. H. Voelcker, "Investigation of porous silicon photocathodes for photoelectrochemical hydrogen production," *Int. J. Hydrogen Energy*, vol. 41, no. 44, pp. 19915–19920, 2016.
- [6] U. Muhsin Nayef, "Fabrication and Characteristics of Porous Silicon for Photoconversion," *Int. J. Basic Appl. Sci. IJBAS-IJENS*, vol. 13, no. 2, pp. 61–65, 2013.